Liquid Crystals
Publication details, including instructions for authors and subscription information:
http://www.informaworld.com/smpp/title~content=t713926090

NMR studies of the ferroelectric SmC* phase

Mario Cifelli[a]; Valentina Domenici[a]; Alberto Marini[a]; Carlo Alberto Veracini[a]
[a] Dipartimento di Chimica e Chimica Industriale, Pisa, Italy

Online publication date: 06 July 2010

To cite this Article Cifelli, Mario , Domenici, Valentina , Marini, Alberto and Veracini, Carlo Alberto(2010) 'NMR studies of the ferroelectric SmC* phase', Liquid Crystals, 37: 6, 935 — 948
To link to this Article: DOI: 10.1080/02678291003784131
URL: http://dx.doi.org/10.1080/02678291003784131

Liquid Crystals,
Vol. 37, Nos. 6–7, June–July 2010, 935–948

Taylor & Francis
Taylor & Francis Group

INVITED ARTICLE

NMR studies of the ferroelectric SmC* phase

Mario Cifelli, Valentina Domenici, Alberto Marini and Carlo Alberto Veracini*

Dipartimento di Chimica e Chimica Industriale, via Risorgimento 35, 56126 Pisa, Italy

(*Received 1 December 2009; accepted 4 March 2010*)

In this work an attempt is made to compare and rationalise the structural and dynamic behaviour of some ferroelectric rod-like mesogens studied by our group in recent years, mainly by means of ^{2}H- and ^{13}C-nuclear magnetic resonance (NMR) spectroscopy. This comparison concerning the local orientational order, the average molecular conformation and the chiral smectic C (SmC*) phase structure, with a brief overview on the reorientational dynamic properties, allowed us to identify some common behaviour of these ferroelectric rod-like mesogens when decreasing the temperature from lower ordered phases to and within the SmC* phase. The main results obtained by means of NMR studies on these mesogens are rationalised and discussed in comparison with detailed discrete Fourier transform computations of their molecular conformations (in the limit of isolated molecules) with the purpose of enlightening the role of intermolecular and packing interactions in the ferroelectric phase with respect to the smectic A and nematic phases.

Keywords: deuterium NMR; carbon-13 NMR; *ab initio* calculations; order parameters; tilt angles; ferroelectric; SmC* phases

1. Introduction

Alfred Saupe become interested in chiral smectics just before his retirement in Halle where, from 1992 until 1997, he was head of the Max Planck Group of Liquid Crystalline Systems at the Martin Luther University, leading studies of electric switching of chiral smectic C (SmC*) phases, new research into bent-core mesogens and the application of atomic force microscopy for the characterisation of liquid-crystalline surfaces. Among his contributions to ferroelectric phases one can find for instance a comprehensive explanation of the layer shrinking induced by the electric field [1], or an interesting investigation about the supramolecular structure of chiral smectic C films with bookshelf alignment [2]. Some of his latest contributions are also related to specific problems of technological applications of ferroelectric liquid crystals (FLCs) [3].

Chiral smectic liquid-crystalline phases have attracted much attention during the last three decades both because of their rich and, in many aspects, fascinating polymorphism, and because of their possible technological applications. Chirality, together with the constraint that mesogenic molecules should pack in layers, is a fundamental factor in creating supramolecular organisations and novel functions of liquid crystal (LC) materials [4]. Scientific and technological interests in FLCs have been reviewed by Lagerwall [5].

Our group in Pisa has been involved in recent years in studies on both the structure and dynamics of several ferroelectric materials using mainly ^{2}H-nuclear magnetic resonance (NMR) and, more recently, ^{13}C-NMR spectroscopy [6]. We should recall here that Alfred Saupe was one of the pioneers of NMR studies of LCs [7]. These NMR studies have been concerned with the structure of either mesogenic molecules or their aggregates [8], as well as the dynamics of molecules in ordered phases and the effect of the magnetic field on the supramolecular structure of chiral smectic phases. NMR has the unique ability to investigate the detailed and site-specific properties of oriented molecules [9], and can provide information on fundamental questions like: what are the molecular structure changes, if any, on passing through phase changes in polyphasic FLC? What is the dependence of the tilt angle on the molecular structure? Can we explain the different response of these materials to the unwinding of the helical structure by external magnetic fields?

Recent progress in density functional methods, moreover, has allowed reliable calculations of molecular structure and relevant tensorial molecular properties (at least for isolated molecules). These calculated properties, such as the ^{13}C chemical shift tensors, in conjunction with NMR techniques, suitably developed to measure ^{13}C chemical shift tensors of individual carbon atoms in molecules, allow us to determine structural and orientational properties of mesogens in LC phases. Can these computations also be of some help in confirming the molecular structural changes within the different mesophases, as observed by means of NMR?

To give even a partial answer to these questions we undertake in this article a comparison between

*Corresponding author. Email: verax@dcci.unipi.it

ISSN 0267-8292 print/ISSN 1366-5855 online

DOI: 10.1080/02678291003784131
http://www.informaworld.com

experimental findings concerning orientational order and the structure of a series of mesogens giving rise to chiral smectic LC so far investigated by NMR spectroscopy, exploiting also the results of discrete Fourier transform (DFT) computations of their structure, in order to have some sort of a reference state undistorted from intermolecular and packing interactions.

2. Experimental and computational details

2.1 Samples and mesomorphic behaviour

The chemical structures of the investigated FLCs (**8BEF5**, **MBHB**, **10B1M7**, **11EB1M7**, **ZLL7/*** and **M10/****) are shown in Figure 1, where seven chiral smectogens of differing molecular complexity are reported. All the compounds share the following general molecular structure: an achiral alkyl (as for **8BEF5** and **MBHB**) or alkyloxy chain (for the other FLCs), a molecular core formed by a biphenyl unit connected to a phenyl unit by an ester group (the order of the connection is the same for **8BEF5**, **MBHB** and **ZLL7/***, while it is reverse for the other smectogens, namely **10B1M7**, **11EB1M7** and **M10/****), and a chiral chain, with one or more chiral centres connected to the core. The stereochemical purity of these compounds is more than 99%, as required for comparative studies. The synthetic details and the macroscopic properties for these compounds are reported elsewhere [10–16].

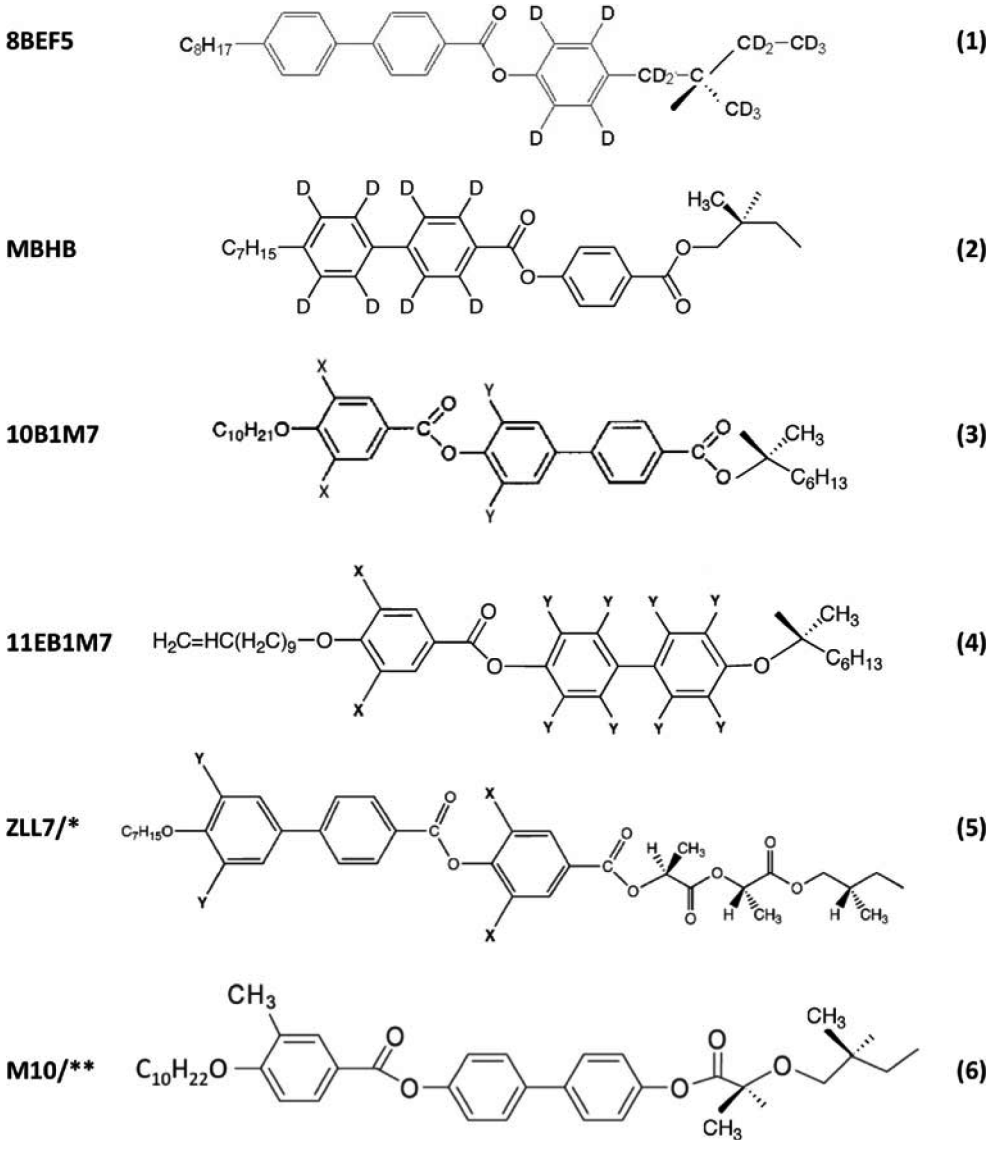

Figure 1. Chemical structures of (1) **8BEF5-phe-d$_{14}$**; (2) **MBHB-biphe-d$_8$**; (3) **10B1M7-phe-d$_2$** (X=D, Y=H) and **10B1M7-biphe-d$_2$** (X=H, Y=D); (4) **11EB1M7-phe-d$_2$** (X=D, Y=H) and **11EB1M7-biphe-d$_8$** (X=H, Y=D); (5) **ZLL7/*** (X=H, Y=H), **ZLL7/*-phe-d$_2$** (X=D, Y=H) and **ZLL7/*-biphe-d$_2$** (X=H, Y=D) and (6) **M10/****.

Table 1. Phase transitions, labelling and transition temperatures of the investigated chiral liquid crystals.

Compound	Labelling	Phases and transition temperatures [°C]
8BEF5	phe-d_2	Cr – 46 – SmG* – 61 – SmJ* – 63 - SmI* – 66 – Sm C* – 78 – SmA – 135 – N* – 136 – BPIII – 137 – I
MBHB	biphe-d_8	Cr – [37.0– SmF* – 53.0] – 58.0 – SmC* – 94.0 – SmA – 162.5 – I
10B1M7	not labelled [12]	Cr – [25.2– SmJ* – 47.8] – 62.5 – SmC^*_A – 69.0 – SmC^*_{ferri} – 75.9 – SmC* – 105.2 – SmA – 124.5 – I
11EB1M7	phe-d_2	Cr – 72.2 – SmI* – 76.9 – SmC* – 91.0 – SmA – 102.0 – TGBA* – 108 – N* – 113.2 – BPI – 115.9 – I
	biphe-d_8	Cr – 63.5 – SmI* – 68.7 – SmC* – 90.3 – SmA – 103.1 – TGBA* – 107.4 – N* – 109.8 – BPI – 111.4 – I
	–	Cr – 51.0 – Hex – 65.0 – SmC^*_{re} – 71.0 – SmC^*_A– 98.0 – SmC* – 104.0 – SmA – 129.0 – I
	phe-d_2	Cr – 51.0 – Hex – 64.0 – SmC^*_{re} – 70.0 – SmC^*_A– 95.0 – SmC* – 101.0 – SmA – 128.0 – I
ZLL7/*	biphe-d_2	Cr – 50.0 – Hex – 62.0 – SmC^*_{re} – 69.0 – SmC^*_A– 93.0 – SmC* – 98.0 – SmA – 127.0 – I
M10/**		Cr – 18.0 – SmC* – 83.0 – N* – 92.0 – BPI – 96.0 – I

The phase transitions, determined by differential scanning calorimetry (DSC), are given in Table 1.

2.2 ^{2}H- and ^{13}C-NMR measurements

Structural, orientational order and dynamic properties of **8BEF5** [10, 17, 18], **MBHB** [11, 19–21], **10B1M7** [12, 21–26], **11EB1M7** [14, 27–32], **ZLL7/*** [15, 32–35] and **M10/**** [16, 36] samples were recently investigated by ^{2}H-NMR and ^{13}C-NMR spectroscopy. ^{2}H-NMR experiments were performed on different NMR spectrometers, which allowed us to study the influence of different magnetic fields strengths (from 4.7 to 9.04 T) on the supramolecular structure of chiral smectic phases of some of the compounds investigated, namely **MBHB**, **11EB1M7** and **ZLL7/*** [19, 32, 37, 38]. Experimental details of the NMR measurements are reported elsewhere [10–38].

2.3 Computational details

The complete molecular structures of **8BEF5**, **MBHB**, **10B1M7**, **11EB1M7**, **ZLL7/*** and **M10/**** were built up using GaussView 3.0, and all the calculations were done with the Gaussian 03 [39] computational package. The geometries of the molecular models were optimised with DFT methods at the B3LYP/6-31G(d) level of theory. In Figure 2 the aromatic cores coming from whole structure optimisation are reported in order to enlighten the structural features of these rigid parts. The magnetic susceptibilities were determined at the DFT level of theory with the modified Perdew-Wang exchange-correlation functional MPW1PW91 [40] and the 6-311+G(d,p) basis set, which seems to be the best compromise between accuracy and CPU time resources. In order to overcome the gauge problem when deriving magnetic properties [41], the Complete Set of Gauge Transformation method [42] was used for calculating the magnetic susceptibilities, analysed using home-made programs written in Mathematica 5.0 software for Apple Macintosh (copyright 1988–2003, Wolfram Research, Inc.).

3. Methodology

NMR spectroscopy is a powerful and versatile means to investigate the structure and dynamics of complex materials [6, 8, 9], and it has been extensively and successfully exploited to investigate different aspects of LCs [43]. In this context, ^{2}H- and ^{13}C-NMR have played and continue to play a relevant role [6, 8, 9, 44, 45]. In particular, while ^{2}H spectra can be exploited to investigate the molecular order and dynamics of selectively deuteriated molecular fragments, ^{13}C-NMR can be a valuable means to gather information on order and structure through the analysis of the Chemical Shift Anisotropy (CSA) for all the carbons in the mesogen [46].

3.1 Order parameters from ^{2}H-NMR

The quadrupolar interactions that dominate the ^{2}H-NMR spectrum are directly related to the orientational order of the deuterium quadrupolar tensor in the LC phase. A detailed theoretical treatment can be found elsewhere [47]; here we just want to recall that for deuteriated aromatic fragments (i.e. phenyl or biphenyl moieties) the quadrupolar splitting measured in the spectrum can be written as [9]

$$\Delta\nu_Q = \frac{3}{2}\omega_Q\left[S_{ZZ}\left(\cos^2\phi - \frac{1}{2}\sin^2\phi - \frac{\eta}{6}\cos^2\phi + \frac{\eta}{6} + \frac{\eta}{3}\sin^2\phi\right) + +\Delta\left(\frac{1}{2}\sin^2\phi + \frac{\eta}{6}\cos^2\phi + \frac{\eta}{6}\right)\right], \quad (1)$$

where S_{zz} and $\Delta = S_{XX} - S_{YY}$ are the principal order parameter and the biaxiality of the deuteriated fragment, ϕ is the angle between the phenyl (or biphenyl) *para* axis and the CD bond with ω_Q and η being the quadrupolar constant and the asymmetry parameter of the quadrupolar interaction, respectively.

Equation (1) can be readily used, with reasonable assumptions (i.e. in the case of CD bonds on aromatic fragments, where ϕ can be assumed to be 60° for

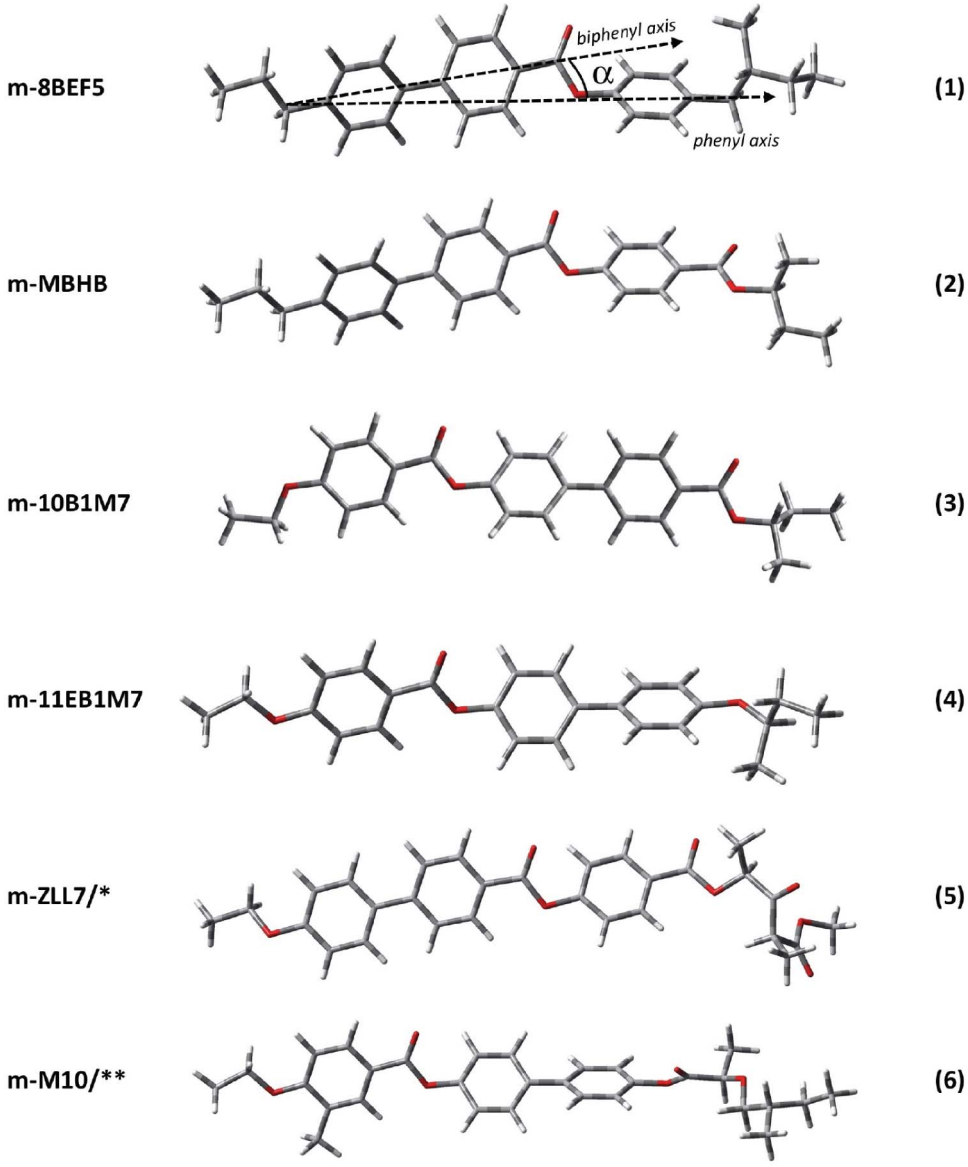

Figure 2. Optimised molecular structures (here the terminal chains have been removed in order to emphasise the structural features of the aromatic cores) of the investigated ferroelectric liquid crystals (the labelling refers to that given in Figure 1). The prefix 'm' refers to 'molecular model', the structural angle 'α' is reported for **m-8BEF5**, together with both the biphenyl and the phenyl *para* axes.

geometric reasons, ω_Q and η can be fixed according to the literature values to 185 kHz and 0.04), to measure orientational order and structural parameters of the phenyl (or biphenyl) moiety in LC phases.

3.2 *Order parameters from ^{13}C-NMR*

For each chemically distinguishable carbon nucleus in the molecule, the temperature-dependent observed chemical shift (δ^{obs}), measured from static ^{1}H-decoupled ^{13}C spectra in uniaxial LC phases, is related to the orientational order parameters through the chemical shift tensor elements (δ_{ab}) by [6]

$$\delta^{obs} = \delta^{iso} + \frac{2}{3}\left[\Delta\delta s_{zz} + \frac{1}{2}\left(\delta_{xx} - \delta_{yy}\right)\left(S_{xx} - S_{yy}\right) + 2\delta_{xz}S_{xz} + 2\delta_{xy}S_{xy} + 2\delta_{yz}S_{yz}\right], \quad (2)$$

where

$$\Delta\delta = \delta_{zz} - \frac{1}{2}\left(\delta_{xx} + \delta_{yy}\right) \quad (3)$$

is the anisotropy of δ with respect to the molecular z-axis, the Saupe ordering matrix $\boldsymbol{S}$ is defined in a molecular (x, y, z) frame, and the tensor $\boldsymbol{\delta}$ is written

in the same frame. δ^{iso} is the isotropic chemical shift (i.e. one-third of the trace of the chemical shift tensor (CST)). The tensor $\boldsymbol{\delta}$ written in the molecular frame can be related to that defined in its principal axis system (PAS) by means of the transformation

$$\delta_{ab} = \sum_{\varepsilon} \cos\theta_{\varepsilon a} \cos\theta_{\varepsilon b} \delta_{\varepsilon\varepsilon}, \qquad (4)$$

where $\theta_{\varepsilon a}$ is the angle between the ε principal axis and the *a* molecular axis. Indeed, the main limitation in employing ^{13}C anisotropic chemical shifts measured from static ^{1}H-decoupled ^{13}C-NMR spectra arises from the need to know the shielding tensor in the molecular coordinate system where the Saupe ordering matrix is defined. This problem can be overcome by means of a combined theoretical and experimental approach, which has been described in detail elsewhere [34, 48, 49]. From the experimental point of view, the principal values of the shielding tensor can be determined by employing 2D high resolution solid state (HR-SS) NMR techniques (e.g. SUPER or PASS). These values can be used to validate the theoretical shielding tensor obtained by DFT calculations on reliable minimum energy conformers. Finally, the orientational order parameters determined from this approach can be further validated by comparison with those previously obtained by an independent ^{2}H-NMR study or by other experimental techniques.

3.3 Tilt angle estimation from NMR determined order parameters

An interesting application of the order parameters determined from NMR is the evaluation of tilt angle θ in the SmC*, first presented by Catalano *et al.* [11]. Tilt angle estimation results from the simple but sound consideration that, as the phase director tilts away from the field direction, the order parameter $S_{ZZ}^{SmC*}(T)$ measured in the tilted phase directly through Equation (1), i.e. referred to the magnetic field direction, can be expressed as

$$S_{ZZ}^{SmC*}(T) = S_{ZZ}^{\hat{n}}(T)\left(\frac{3}{2}\cos^2\theta - \frac{1}{2}\right), \qquad (5)$$

where $S_{ZZ}^{\hat{n}}(T)$ is the main order parameter with respect to the director, **n**.

When spectra are acquired in magnetic fields strong enough to unwind the chiral helical structure, the director, as well as the molecules, are aligned with respect to the magnetic field ($\theta = 0$) and $S_{ZZ}^{\hat{n}}(T)$ can be measured directly from the quadrupolar splittings measured in the unwound SmC* phase. If ^{2}H-NMR measurements at lower fields are available, where the SmC* phase has an unperturbed helical structure (and $\theta \neq 0$), the $S_{ZZ}^{SmC*}(T)$ can be determined [19, 32, 37] and the tilt angle θ can be found from the ratio $S_{ZZ}^{SmC*}(T)/S_{ZZ}^{\hat{n}}(T)$ via Equation (5).

In the case where a direct measurement of $S_{ZZ}^{\hat{n}}(T)$ is not feasible (no unwound SmC* phase is obtained even at high magnetic fields), its value can be determined by extrapolating the order parameter behaviour from the smectic A (SmA) phase in the SmC* temperature range, and again Equation (5) can be used [14, 32].

3.4 Structural and NMR parameters from ab initio calculations

The recent achievements in *ab initio* – first principles methods, computer hardware and software have made it possible to obtain accurate molecular structures (e.g. energies, conformational distributions, etc.), and to evaluate many response properties precisely (e.g. IR and Raman frequencies, UV-vis and fluorescence spectra, relevant NMR tensorial quantities such as the chemical shielding, scalar and quadrupolar coupling tensors). In particular, as for ^{13}C CSA analysis the main limitation results from the need to know the shielding tensor orientation in a molecular coordinate system, this difficulty can be quite straightforwardly overcome by using quantum mechanical calculations, performed to obtain (i) optimised geometries from the potential energy surface of the molecular models investigated, (ii) the orientation and the principal components of the relevant chemical shielding tensors, (iii) the dependence of CSTs on both structural parameters and conformational states and, when possible, (iv) the influence of the surrounding molecules on that investigated [41].

3.5 Dynamic properties in the ferroelectric phases from ^{2}H T_{1Q} and T_{1Z} relaxation times

The quantitative analysis of the deuterium longitudinal relaxation times (T_{1Q} and T_{1Z}) in the LC phases is now a state-of-the-art method when it is applied to uniaxial phases, such as nematic and SmA phases, formed by low molecular weight rod-like mesogens. The details of the theoretical approaches to the extraction of the dynamic information from the relaxation times have been reviewed elsewhere [6, 43, 45, 50]. The quantitative analysis of relaxation times for biaxial mesophases, such as the SmC*, is much more complicated due to several difficulties in linking the measured relaxation times to the dynamic parameters. As

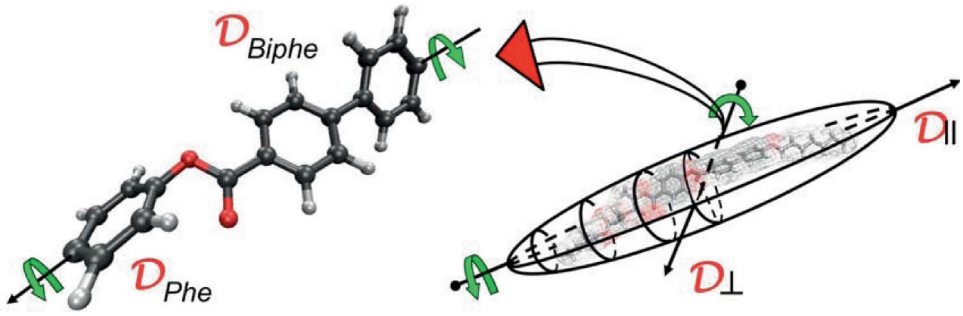

Scheme 1. Representation of the rotational diffusion motions: overall, spinning ($D_{\parallel}$) and tumbling ($D_{\perp}$), and internal rotation around the phenyl (D_{phe}) and biphenyl (D_{biphe}) principal axes.

reported by Domenici *et al*. [18], the complications are both theoretical and experimental, partially due to the phase biaxiality, and as a consequence of the introduction of many parameters, and to the dependence of the relaxation times on the polar angles defining the position of the local director with respect to the external magnetic field. The approach proposed by Domenici *et al.* [18] is based on the assumption of uniaxiality of the helical supramolecular structure, thus discarding the effect of the azimuthal angle, but taking into account the effect of the tilt angle on the spectral densities. In this way it is possible to determine the reorientational diffusion coefficients for the overall molecular motions, namely spinning ($D_{\parallel}$) and tumbling ($D_{\perp}$) rotations, as well as the internal rotational diffusion coefficients (D_R) of the deuterium-labelled fragments (see Scheme 1).

4. Discussion

This section is divided in five parts, each dealing with specific properties of the ferroelectric SmC* phase and their molecular constituents, as determined by means of a multinuclear ^{2}H- and ^{13}C-NMR approach integrated with *ab initio* calculations. They are (1) local and molecular order; (2) the angle between the fragments of the aromatic core; (3) the tilt angle of the SmC* phase; (4) the effect of the magnetic field; and (5) fast molecular diffusion in the ferroelectric phase. In order to provide a general description and validation of the approach proposed previously, several examples of FLCs are reported here and commented on because they can be then considered as representative cases.

The SmC* phases of **8BEF5** [10, 17, 18] and **MBHB** [19–21] have been studied by means of ^{2}H-NMR in a single aromatic fragment (phenyl for the first and biphenyl for the latter, respectively). In the case of **8BEF5**, the ^{13}C-NMR has also been employed to determine molecular order parameters in its chiral phases. Moreover, **MBHB** represents the first case where different behaviour observed at different magnetic field strengths allowed a consistent determination of the tilt angle, θ, by using the methodology of unwinding the chiral helix, as described in Section 3.3. The molecular dynamics in the SmA and SmC* phases of these two mesogens were also investigated by means of ^{2}H-NMR longitudinal relaxation measurements in the MHz region.

Three widely investigated samples are the smectogens **10B1M7** [12, 21–26], **11EB1M7** [14, 27–32], and **ZLL7/*** [15, 32–35, 38], where two isotopomers selectively deuterium labelled on the phenyl and biphenyl moieties were available (see Figure 1). This allowed us to determine the local orientational order of the two fragments and the relative angle α between them, as presented in Section 4.2. The effect of the magnetic field on the chiral phases of **11EB1M7** and **ZLL7/*** was also investigated by means of ^{2}H-NMR spectroscopy. Moreover, for these two mesogens, a detailed analysis of the ^{2}H T_{1Q} and T_{1Z} relaxation times in the SmA and SmC* phase allowed us to obtain reliable values of the rotational diffusion coefficients not only for the overall molecular reorientations but also for the internal reorientations of the phenyl and biphenyl moieties, thus giving a significant view of the internal dynamics when passing from the SmA to the ferroelectric SmC* phase. For **ZLL7/***, a complete comparative ^{2}H-, ^{13}C-NMR and *ab initio* calculation approach was applied, thus representing an important test for validating the overall methodology.

The **M10/**** ferroelectric sample has been studied by combining *ab initio* calculations and ^{13}C-NMR spectroscopy [16, 36]. This case is reported here in view of a comparison among FLCs concerning the orientational order parameter and the effect of lateral substituents on the aromatic core on the molecular orientational properties.

4.1 *Local and molecular order*

The analysis of both quadrupolar and dipolar (where available) splittings as determined from ^{2}H-NMR

spectra allows us to obtain the local orientational order parameters of the labelled moieties. For the aromatic deuterons of the phenyl and biphenyl fragments both main local order parameter, S_{zz}, and fragment biaxiality, Δ_{biax}, can be determined (see Equation 1). The values and/or ranges of these local order parameters, as obtained for the deuteriated samples **8BEF5, MBHB**, **10B1M7**, **11EB1M7** and **ZLL7/*** in their SmC* phase, are reported in Table 2.

It should be noted that, for simplicity, we have reported only the values of S_{zz} as obtained at the higher magnetic field, since in some cases the ^{2}H-NMR spectra were recorded at several magnetic field strengths. This is rather crucial because, in some of the mesogens studied, the magnetic field used in NMR experiments was strong enough to unwind the helical structure of the SmC* phase; this will be addressed in detail in Section 4.4. For instance, as can be seen in Table 2, the values of S_{zz} for the **MBHB** sample increase on decreasing the temperature, reaching a very high value (0.92) due to the fact that the helix of the SmC* phase is totally unwound and the local director **n** and the molecules are parallel to the magnetic field. In this case we have direct access to $S^{n}_{ZZ}(T)$. In contrast, for instance, the SmC* phase of the **8BEF5** sample is not unwound by the field, and the values of S_{zz} reported in Table 2 decrease on decreasing the temperature. In this case we have access to the $S^{SmC*}_{ZZ}(T)$ quantity which includes the effect of the tilt angle, θ, through the factor $\left(\frac{3}{2}\cos^2\theta - \frac{1}{2}\right)$. For the complexity and variety of the cases examined, it is rather difficult to extrapolate a general trend or range of typical values for S_{zz} in the SmC* phase. This fact is also due to the different temperature ranges of stability of the SmC* phase for the different mesogens, as well as to the presence of SmA or chiral nematic (N*) phases at higher temperatures. However, several analogies could be cited:

(i) One observation concerns the local order of the aromatic fragment connected to alkyl chains (as for **8BEF5** and **MBHB**), which is always higher than that found for those connected to alkoxyl chains (as for **10B1M7**, **11EB1M7** and **ZLL7/***).

(ii) Another interesting feature concerns the low value of biaxiality of fragment ordering, which is, in the highest case, about 0.05 for the phenyl ring of **ZLL7/*** and **10B1M7**. This experimental evidence is also confirmed from the local dynamics of these fragments which is usually fast, thus indicating a rapid rotation with respect to their *para* axes, also in the ferroelectric phase, as shown in Section 4.5.

(iii) Another aspect which is demonstrated by the three cases where two selectively deuteriated isotopomers were available (**11EB1M7**, **ZLL7/*** and **10B1M7**) concerns the local ordering of the two fragments and their relative orientation in the magnetic field. In fact, in these three cases, the aromatic fragments connected to the non-chiral chains (thus far from the chiral moieties) are more ordered than those directly connected to the chiral part of the molecule. For instance, the cases of **11EB1M7** and **ZLL7/*** can be taken as representative. In both of these, two isotopomers were available, and the analysis of ^{2}H-NMR spectra allowed us to obtain the orientational ordering properties of the two aromatic fragments independently. As shown in Table 2, the most ordered fragment is the phenyl ring for the **11EB1M7** sample and the biphenyl moiety for the **ZLL7/*** sample. This behaviour has two exceptions, at least among the cases reported in this work: (a) the **M10/**** sample, where the biphenyl unit, which is connected to the achiral chain, is more ordered than the phenyl one – however, in this mesogen the phenyl unit has a methyl substituent in the ortho position, which dramatically increases its local order biaxiality [36] (note that in Table 2 only the molecular order parameters are reported); and (b) the

Table 2. Orientational order parameters of the investigated compounds, studied by ^{13}C-NMR on the unlabelled compound and by ^{2}H-NMR on the corresponding deuteriated isotopomers in the SmC* phase. The order parameters reported here refer to those determined from the relevant NMR parameters (e.g. dipolar and quadrupolar splittings, chemical shift anisotropies) measured at the highest magnetic field.

Compound	^{13}C-NMR S_{zz} (LC)	^{13}C-NMR Biax (LC)	^{2}H-NMR S_{zz} (phe)	^{2}H-NMR Biax (phe)	^{2}H-NMR S_{zz} (biphe)	^{2}H-NMR Biax (biphe)	Most ordered
8BEF5	0.87–0.83	~ 0.12	0.85–0.81	~ 0.03	—	—	—
MBHB	—	—	—	—	0.82–0.92	~ 0.02	—
10B1M7	0.76–0.65	~ 0.06	0.73–0.64	~ 0.05	0.64–0.51	~ 0.00	**phe**
11EB1M7	—	—	0.67–0.66	~ 0.04	0.68–0.60	~ 0.03	**phe**
ZLL7/*	0.68–0.71	~ 0.06	0.72–0.73	~ 0.05	0.73–0.75	~ 0.00	**biphe**
M10/**	0.88–0.92	~ – 0.26	—	—	—	—	**biphe**

8BEF5 sample, where the deuteriated phenyl ring is linked to the chiral chain directly through a CC bond, thus justifying the higher order.

The order parameters obtained by analysing the ^{13}C-NMR chemical shift data [34] for **8BEF5**, **10B1M7** and **ZLL7/*** agree with those obtained by the independent ^{2}H-NMR study. In particular, the comparison between ^{2}H- and ^{13}C-NMR results, reported for **ZLL 7/*** [34], is also important because it validates the common assumption for which the main orientational order of the aromatic core (or of the more ordered aromatic moiety) can be considered nearly coincident with the main molecular order parameter [34]. In this case, the structural and orientational ordering properties of **ZLL 7/*** were determined by exploiting the chemical shielding properties of ^{13}C nuclei. To this aim, solid-state NMR techniques such as CP, SPINAL-64 and SUPER were employed to record static ^{13}C-$\{^{1}$H$\}$ NMR spectra and 2D CSA powder patterns, respectively, in combination with DFT calculations used to obtain directly the CST values and their orientations in the PAS frame.

Differently, in the case of **M10/**** only the calculated in vacuum GIAO-DFT chemical shielding tensors and orientations were available (2D solid-state NMR measurements are currently in progress in our group) [36]. Therefore, the structural and orientational order analyses were made by applying Equations (3) and (4) to the experimental ^{13}C chemical shift anisotropies previously measured and reported [16]. The S_{zz} and Δ_{biax} values reported in Table 2 were found to be higher than those commonly determined for other FLCs. In particular, the very high value of Δ_{biax} seems to depend on the particular molecular structure of **M10/****, where the biphenyl unit is connected to the chiral chain and, more important, one methyl unit is attached directly to the phenyl core (see Figure 1(6)), thus rendering it more biaxial than a normal phenyl connected to the longest aliphatic chain [36]. Generally, even though ^{13}C-NMR presents a more complex route than ^{2}H-NMR, the results obtained for **M10/****, as previously found for **ZLL7/***, suggest that the recent progress in both theoretical and experimental techniques can allow the determination of reliable structural and ordering information. This overcomes not only the problem of synthesising suitably deuteriated compounds, but might also allow the detailed study of molecular moieties (such as ester groups) inaccessible to ^{2}H-NMR.

4.2 Angle between fragments of the aromatic core

The estimation of the average angle between the two principal axes of the two aromatic fragments can be performed by comparing the main local orientational order parameter, S_{zz}, of two fragments of the same molecule. The term 'average' implies that these fragments can be connected by a flexible or semi-flexible link (as for the ferroelectric systems reported in this work) which determines the relative motion of the two parts. These internal motions, which can be related to fast conformational changes, cannot be resolved in the ^{2}H-NMR characteristic time and the result is an averaged quantity. However, all this considered, the comparison between the local orientational order of different fragments, such as the phenyl and biphenyl moieties, can be used to obtain the average angle between the two *para* axes as a function of temperature, and this can be rather informative especially when compared with that of other mesogens in the same mesophase.

As far as the ^{2}H-NMR measurements are concerned, the values of the angle α are determined at each temperature since S_{zz} for the two fragments is available at these temperatures (if two different isotopomers are investigated). In this case, we can obtain the temperature variation of this structural property, as done for **10B1M7**, **11EB1M7** and **ZLL7/*** (see Figure 3). In the case of ^{13}C-NMR, the angle α is determined from the local order parameters for the two aromatic fragments, derived from the self-consistent analysis of the ^{13}C- chemical shift anisotropies measured in the unlabelled sample.

In all cases, the angle between the two fragments has also been determined in the other phases. In particular, in the SmA phase of **11EB1M7** and **ZLL7/*** this angle increases rapidly with decreasing temperature. In the SmC* phase, the angle remains almost constant, while for **ZLL7/***, where data at lower temperatures are available, it continues to increase until the hexatic phase is reached. For **10B1M7** the value of this angle was found to fluctuate more strongly, especially within the ferro(ferri/antiferro)-electric phases. These experimental trends can be understood with the help of *ab initio* calculations (see Table 3). The structural angle α extracted from DFT calculated for *in vacuo* minimum energy conformers of the investigated molecules is in very good agreement with those extracted from both ^{2}H- and ^{13}C-NMR analyses if we limit comparison to the SmA phase. Moreover, the angle α exhibits a more pronounced temperature dependence in the case of SmA phases compared with SmC* phases. This may be due to the presence of a progressive reduction of conformational freedom already in the SmA phase. It is worth noting that our findings are in complete agreement with the theoretical model proposed by Photinos and Samulski [51] concerning the conformational changes at the SmC*–SmA transition. In fact, the dramatic change in the trend of the angle between two fragments at a certain temperature can be related to a conformational change, and the comparison with

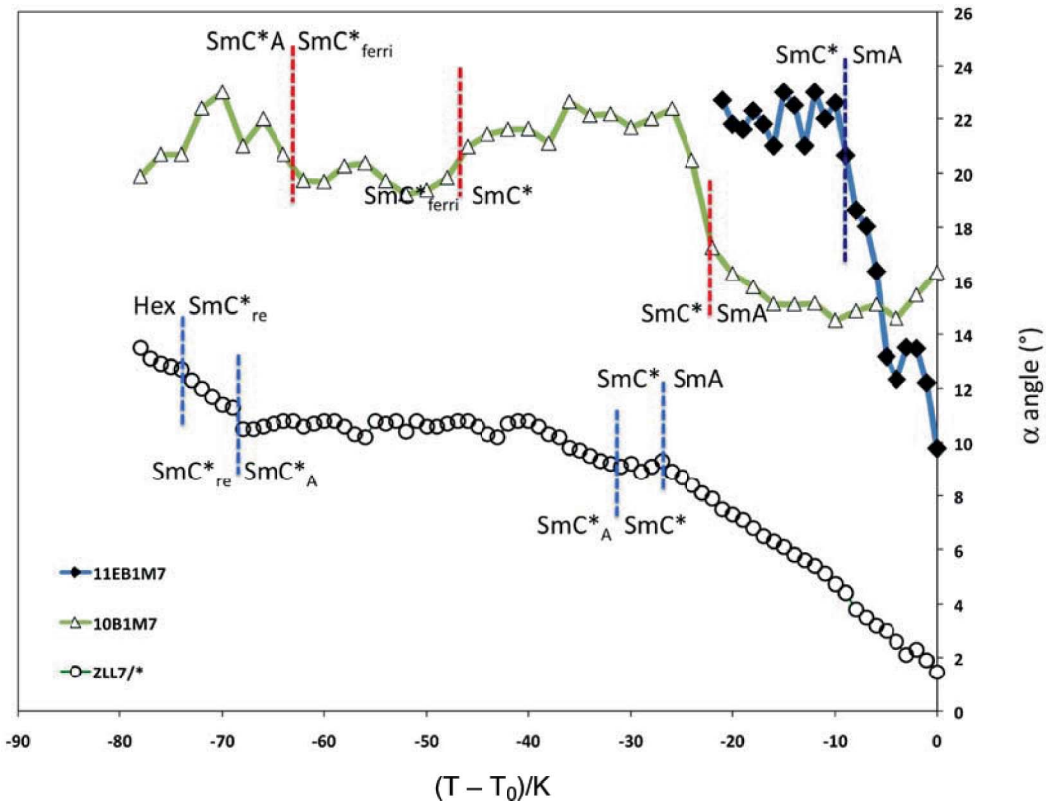

Figure 3. Temperature trends of the structural angle α (the angle between the phenyl and biphenyl axes), evaluated by ^{2}H-NMR for **10B1M7**, **11EB1M7** and **ZLL7/*** mesogens. Note that T^0 is the SmC*–SmA transition temperature.

Table 3. The values of the structural angle, α, calculated at DFT level (see computational details) are reported together with those determined by NMR, in the SmA, SmC* and SmC^*_A, as explained in the text.

	DFT	^{2}H-NMR			^{13}C-NMR		
Compound	(vacuo)	SmA	SmC*	SmC^*_A	SmA	SmC*	SmC^*_A
8BEF5	8.2	—	—		—	—	
MBHB	8.6	—	—		—	—	
10B1M7	13.5	14–17	20–23	20–23	14.4	—	—
11EB1M7	12.8	10–18	20–24		11.7	—	
ZLL7/*	8.5	2–9	8–9	9–10	5–9	7–8	8–9
M10/**	11.3		—			10–12	

calculated optimised geometries of the mesogenic molecules can be used to confirm this hypothesis [32–34, 38].

4.3 Tilt angle in the SmC phase*

As reported in Section 3.3, there are several possibilities for the evaluation of the molecular tilt angle θ from ^{2}H-NMR measurements. In recent work [10, 12, 14, 19, 32, 38] these methods, based either on the extraction of the trend of S_{zz} from the higher temperature phases or on the comparison between the trends of S_{zz} measured at the highest and lowest magnetic fields (through Equation (5)), have been applied to **8BEF5**, **10B1M7**, **MBHB**, **11EB1M7** and **ZLL7/***. In fact, in these cases the ferroelectric SmC* phase follows the SmA, where the director aligns along the magnetic field direction. This allowed us to extrapolate a trend of S_{zz} directly from the SmA phase ($S^{\hat{n}}_{ZZ}(T)$) and then compare it with that obtained through Equation (1) from the measured quadrupolar splittings in the SmC* phase ($S^{SmC*}_{ZZ}(T)$). We notice that in all the cases investigated, the tilt angle increases continuously, starting from values of 4°–12° at the phase transition (SmA–SmC*) and reaching saturation values of 10°–28° (see Figure 4).

However, for **MBHB**, **11EB1M7** and **ZLL7/*** we have observed the phenomenon of the unwinding of the helix [32] when increasing the magnetic field above a critical value. This finding and, in particular, the comparison among the different trends in S_{zz} at different magnetic fields (typically in the range of 2–10 T), provided a direct proof of the validity of the extrapolation

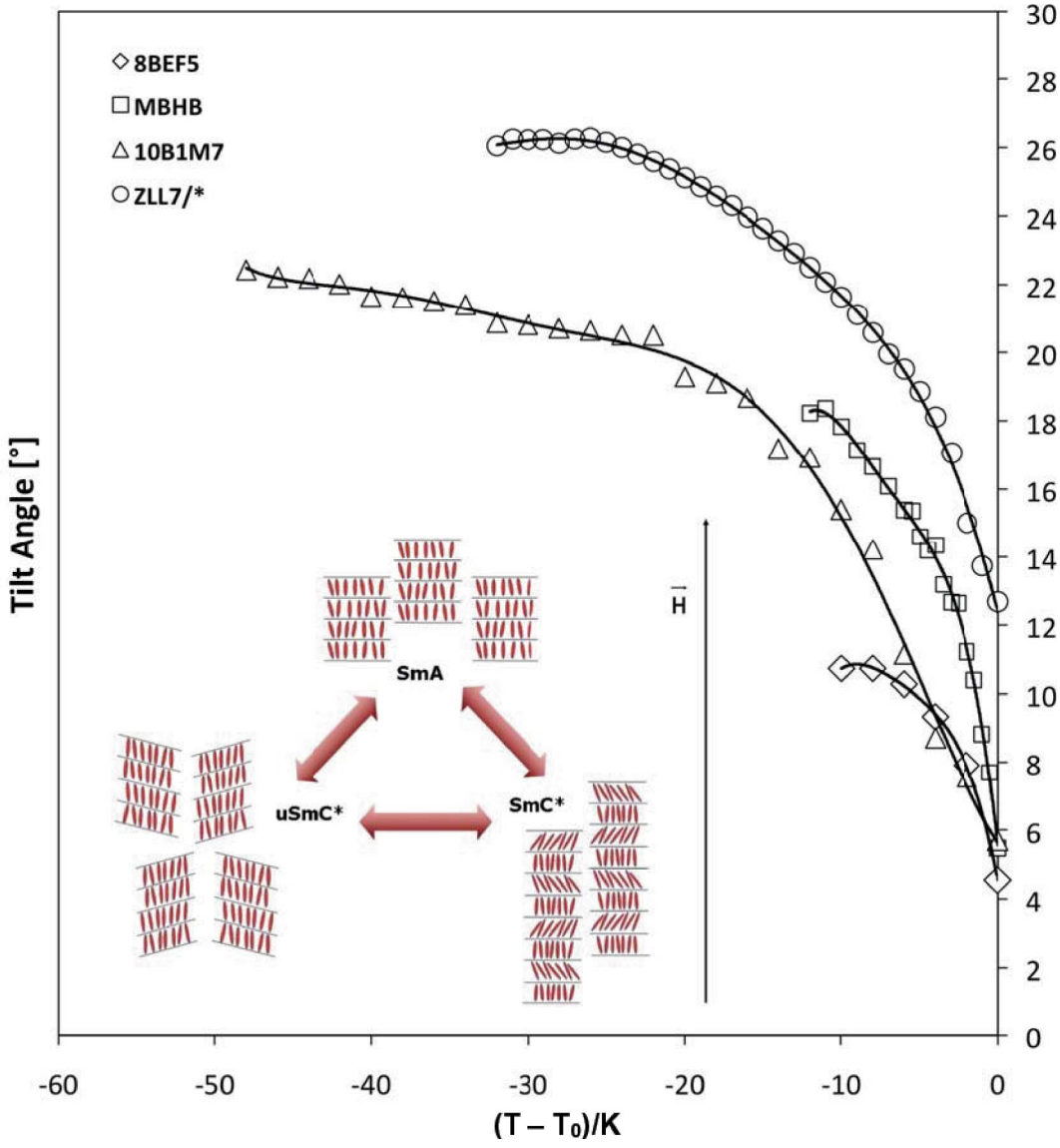

Figure 4. Temperature trends of the tilt angle θ in the tilted phases of **8BEF5**, **MBHB**, **10B1M7** and **ZLL7/*** determined by ^{2}H-NMR, as explained in the text. A sketch of the SmA, SmC* and (unwound) uSmC* phases is reported in the inset (the magnetic field is in the vertical direction, thus parallel to the director of the uSmC* phase and perpendicular to the smectic planes in the SmC* phase). Note that T^0 is the SmA–SmC* transition temperature.

procedure. In fact, in all of these three cases the tilt angle, evaluated by means of Equation (5) with the two methods, was found to be the same, within the experimental error. In Figure 3, the trends of the tilt angle θ obtained from the NMR experiments are reported together with the curve obtained by fitting the experimental data with the Landau–de Gennes equation:

$$\theta = \theta_0 \left[\frac{T_0 - T}{T_0}\right]^{\gamma}, \qquad (6)$$

where T_0 is the SmA–SmC* transition temperature and the parameters γ and θ_0 are specific for each mesogen.

4.4 The effect of the magnetic field

It is well-known that the helical supramolecular structure typical of the ferroelectric SmC* phase can be unwound by applying external electric fields, and this aspect has been investigated in order to design appropriate technological devices. In contrast, the effect of magnetic fields [52] has been less studied, even though it should show similar interesting features. For this purpose, NMR spectroscopy has the advantage of working in the presence of magnetic fields of high intensity, with the possibility to explore different geometrical orientations between the helix axes of the SmC* phase and the magnetic field. The first angular

study of helix unwinding by the magnetic field interaction in the SmC* phases of a ferroelectric smectogen (namely DOBAMBC) was reported by Zalar *et al.* [53]. In their work the authors clearly showed an angular dependence for the critical unwinding field on the angle β, between the helix axis and the magnetic field direction.

The first example of unwinding the helix of the SmC* phase by a magnetic field at β=0 was observed for **MBHB**, and this experimental observation was a stimulus in developing a theoretical model, based the Landau–de Gennes theory, to describe the dependence of the transition temperatures SmC*–SmA, uSmC*–SmA and SmC*–uSmC* by the magnetic field [19, 37]. However, recent NMR investigations on different smectogens, namely **11EB1M7**, **ZLL7/*** [32] and **M10/**** [16], have suggested that the unwinding of the helical structure of the SmC* phase with the magnetic field parallel to the helical axes is a general feature, not specific for **MBHB**, and that the value of the critical magnetic field is in the range of 2–20 T, typical of NMR instruments. These studies, however, showed that the critical magnetic field for unwinding the SmC* helix is strictly related to the specific materials (for instance, through the elastic constants K and the anisotropic magnetic susceptibility Δ_χ) and possibly to some molecular properties.

One of the most interesting aspects in FLC, in fact, is to understand how the mesogenic molecules are organised and packed in the bulk phase (especially in the SmC*) and in the presence of a magnetic field. Knowledge of the anisotropy part, $\Delta\chi^{\mathrm{Mol}}$, of the molecular magnetic susceptibility $\boldsymbol{\chi}^{\mathrm{Mol}}$ of the molecule is necessary for the determination of how the molecular director(s), especially in the case of a SmC* phase in its wound and unwound forms, aligns in a magnetic field. Usually, the magnetic field is not strong enough to orient a single molecule or isolated molecules; in fact the interaction energy, due to cooperative molecular ordering, is indeed crucial [54]. Moreover, in bulk LCs the molecular magnetic susceptibility is significantly different from the phase magnetic susceptibility, which is a quantity averaged over all (anisotropic) motions of the molecules in the LC phase. However, the symmetry properties of the molecular magnetic susceptibility tensor can help in understanding the differences (if there are any), at a molecular level, between chiral smectogens (as those investigated in this paper) and simpler calamitics (such as 5CB or 5OCB) which exhibit nematic phases. At a macroscopic level, the magnetic energy density of the system can be expressed as $g_M = -\Delta\chi(\boldsymbol{B}\cdot\boldsymbol{n})^2/(2\mu_0)$ where μ_0 is the universal permittivity in vacuum, and $\Delta\chi$ is the anisotropic magnetic susceptibility, defined as $\chi_{||} - \chi_\perp$, with $\chi_{||}$ and $\chi_\perp$ denoting the components of the phase magnetic susceptibility tensor parallel and perpendicular to the director, respectively. The direction of preferred alignment of a system in the magnetic field depends on the sign of the anisotropy. Positive $\Delta\chi$ values seen in most LCs result in the alignment of the phase director $\boldsymbol{n}$ parallel to the magnetic field $\boldsymbol{B}$; in contrast, a negative $\Delta\chi$ can often be easily seen in discotic and calamitic LCs constructed only of aliphatic parts. In principle, it is possible to relate the macroscopic property $\Delta\chi$ to the molecular property $\Delta\chi^{\mathrm{Mol}}$ [$\Delta\chi^{\mathrm{Mol}} = \chi_{\|}{}^{\mathrm{Mol}} - \chi_\perp{}^{\mathrm{Mol}} = \chi_{11}{}^{\mathrm{Mol}} - 1/2(\chi_{22}{}^{\mathrm{Mol}} + \chi_{33}{}^{\mathrm{Mol}})$, where $\chi_{11} \geq \chi_{22} \geq \chi_{33}$] as well as the Saupe order parameter, S [55].

As far as the molecular magnetic susceptibility anisotropy is concerned, the investigated FLCs show values of $\Delta\chi^{\mathrm{Mol}}$ ranging between 80 and 90 cgs-ppm ($\Delta_\chi{}^{(\mathrm{SI})} = 4\pi^* \Delta_\chi{}^{(\mathrm{cgs})}$, while ppm $= 10^{-6}$), which are two times greater than those found for 5CB and 5OCB (30–40 cgs-ppm). Moreover, the asymmetry $\eta_\chi{}^{\mathrm{Mol}} = (\chi_{33}{}^{\mathrm{Mol}} - \chi_{22}{}^{\mathrm{Mol}})/(\chi_{11}{}^{\mathrm{Mol}} - \chi_{\mathrm{iso}}{}^{\mathrm{Mol}})$ of the calculated magnetic susceptibility ranges between 0.15 and 0.34, comparable with those found for 5CB and 5OCB (0.15–0.25). All of this considered, from the magnetic susceptibility point of view, the examined FLCs are very similar to the uniaxial calamitic LCs.

4.5 Fast molecular diffusion in the ferroelectric SmC phase*

In order to complete our overview on the molecular properties of ferroelectric mesogens, it is worth noting that in recent years several new results have been reported on the molecular dynamics of these molecules in the fast motion regime (i.e. the MHz region). In particular, the quantitative analysis of longitudinal relaxation times (T_{1Z} and T_{1Q}) [18] allowed us to obtain the trends of molecular rotational diffusion coefficients for some of these mesogens (namely, **8EBF5**, **MBHB**, **11EB1M7** and **ZLL7/***) in their ferroelectric phase and to compare them with those for the high temperature SmA phase. The main results are summarised in Tables 4 and 5, and some general remarks can be given here:

(1) The activation energies of the overall and internal molecular motions in the SmC* phase are usually different from those in the high temperature SmA phase. This fact determines a different slope in the trend of the diffusion coefficients as a function of temperature when passing from SmA to the SmC* phases.
(2) In a few cases, and in particular for the tumbling motion, in addition to a different value of the activation energy we have also observed a discontinuity, or a jump, at the SmC*–SmA transition.

Table 4. Rotational diffusion coefficients and activation energies for the spinning, tumbling and internal motions, determined from ^{2}H-NMR data analysis for several rod-like smectogens in the SmA phase. The values of **D** are taken at a temperature in the middle of the temperature range of stability of the SmA phase.

	Diffusion coefficient			Activation energy ΔE_a/kJ mol^{-1}		
Mesogens	$D_{//}$/s^{-1}	$D_{\perp}$/s^{-1}	D_R/s^{-1}	(//)	($\perp$)	(*R*)
8BEF5-phen-D_4 [18]	7.9×10^8	1.1×10^8	1.9×10^{10}	29.6	29.6	33.3
MBHB-biph-D_8 [20]	2.5×10^9	5.0×10^8	3.2×10^9	32.1	32.1	29.1
11EB1M7-phen-D_2 [28]	1.5×10^9	1.3×10^8	1.5×10^9	35.0	40.0	35.0
11EB1M7-biph-D_2 [28]	1.5×10^9	1.3×10^8	3.5×10^9	35.0	40.0	20.0
ZLL/7*-phen-D_2 [35]	2.0×10^9	4.7×10^7	1.6×10^8	42.44	44.97	45.87
ZLL/7*-biph-D_2 [35]	2.0×10^9	4.7×10^7	1.1×10^9	42.44	44.97	42.82

Table 5. Rotational diffusion coefficients and activation energies for the spinning, tumbling and internal motions, determined from ^{2}H-NMR data analysis for several rod-like smectogens in the SmC* phase. The values of **D** are taken at a temperature in the middle of the temperature range of stability of the SmC* phase.

	Diffusion coefficient			Activation energy ΔE_a/kJ mol^{-1}		
Mesogens	$D_{//}$/s^{-1}	$D_{\perp}$/s^{-1}	D_R/s^{-1}	(//)	($\perp$)	(R)
8BEF5-phen-D_4 [18]	1.0×10^9	1.1×10^8	7.2×10^9	70.0	70.0	19.0
MBHB-biph-D_8 [20]	1.2×10^9	2.3×10^8	1.1×10^9	52.0	52.0	36.0
11EB1M7-phen-D_2 [28]	1.2×10^9	1.1×10^7	4.1×10^8	20.0	119.0	78.0
11EB1M7-biph-D_2 [28]	1.2×10^9	1.1×10^7	1.5×10^9	20.0	119.0	61.0
ZLL/7*-phen-D_2 [35]	7.8×10^8	2.7×10^7	4.6×10^8	42.52	46.58	50.89
ZLL/7*-biph-D_2 [35]	7.8×10^8	2.7×10^7	8.5×10^8	42.52	46.58	41.99

This is particularly evident for **11EB1M7** [27] and **ZLL7/*** [35].

(3) When the deuterium labelling involves both phenyl and biphenyl fragments, it is also possible to note a different behaviour of the diffusion coefficients for these two moieties of the aromatic core when passing from the SmC* to the SmA phase. For instance, in **ZLL7/*** at the SmC*–SmA transition the biphenyl fragment rotates faster (i.e. the activation energy decreases in the SmC* phase), while the phenyl rotates slower (i.e. the activation energy increases in the SmC* phase). It is worth noting that the phenyl and biphenyl fragments have different degrees of local order (higher in the biphenyl one), and this can be related to the relative position of the two fragments with respect to the chiral chain (see Figure 1(5)), as reported in Section 4.1.

(4) In a few cases, such as **MBHB** [20] and **ZLL7/*** [35], it was also possible to determine the rotational diffusion coefficients in the unwound state of the SmC* phase, under the effect of the magnetic field. Surprisingly, these diffusion coefficients are appreciably different between the SmC* and uSmC* phases, thus suggesting that a strong effect due to the changes in the supramolecular structures in these two phases occurs also at the molecular level.

A further general comment is related to the importance of these dynamic investigations in view of our attempt to find a relationship between the molecular properties and the mesophases shown by this class of compounds. Even though our studies mainly focus on fast motions, namely motions active in the MHz frequency region where ^{2}H T_1 relaxation times show higher sensitivity, we can safely state that the transition from a SmA phase to the ferroelectric phase is associated with a change in the internal and overall molecular diffusion motions and that, in most of the cases examined, these changes (either discontinuities at the SmC*–SmA transition and/or changes in the activation energies between the two phases) correspond to analogous variations in terms of local orientational order and conformational features.

However, it should be mentioned that the ferroelectric phase is characterised not only by fast single molecular motions, such as reorientational ones, but also by other processes which can be studied by different NMR techniques, not reviewed here. Several studies on the same mesogens reported here, namely **10B1M7**, **8BEF5** and **ZLL7/***, have been published suggesting that the SmC* phase shows typical motional processes active in the slow regime of motions [26], such as slow translational diffusion within the smectic layer or between the adjacent layers [25] as well as slow collective motions, well determined by multifrequency T_1 [27, 28, 56] and T_2 NMR studies [35].

5. Conclusions

^{2}H- and ^{13}C-NMR are clearly very powerful techniques for the investigation of structural, orientational and

dynamic properties of mesogenic molecules in complex chiral smectics. The information can be detailed and site specific, from a molecular point of view. The deuteriation of some parts of the mesogenic molecules, necessary for ^{2}H-NMR, is still a strong limiting factor because of the synthetic effort needed for isotopic enrichment. With ^{13}C- methods the information is, in principle, available for all carbons in the molecule, even if more difficult to obtain. Few examples are available where these experimental techniques, ^{2}H- and ^{13}C-NMR, have been used in combination. Additionally, DFT computational methodologies offer the possibility to calculate molecular properties, such as conformational and magnetic ones, which can be very useful for the interpretation of NMR data.

In our studies, we have focused mainly on the aromatic core of the investigated ferroelectrics, which reasonably mimics the overall molecule, in particular for the orientational ordering properties. In this context, some interesting points concern the indication of a change in the conformational properties of these mesogens when passing from the low temperature SmC* phase to the high temperature SmA phase. This can be further rationalised in terms of molecular packing and increase of conformational freedom on going from the ferroelectric to the SmA phase. The molecular changes, which can be deduced from the trend of the angle α between the phenyl and biphenyl moieties, as well as the change in local orientational order of these fragments, are in agreement with the slowing down of the reorientational motions affecting either the overall molecules and the aromatic moieties, as obtained from the analysis of ^{2}H longitudinal relaxation times. However, it should also be noted that both the achiral and chiral chains certainly play a fundamental role in determining the mesophase transitions. For this reason, new efforts are needed in order to include in the orientational order investigations the effect of conformational averaging, also taking into account the contribution of flexible chains.

Moreover, we have shown that unwinding of the helical supramolecular structure by magnetic fields, which can easily be explored by means of ^{2}H-NMR spectroscopy, is a general phenomenon in FLCs. For instance, for the mesogens examined, these studies revealed that the unwinding of the helical structure of the SmC* phase depends on a critical magnetic field strength in the range of 2–20 T. The critical field depends in turn on a series of parameters, specific for the investigated material (such as the anisotropic magnetic susceptibility), which can be related to molecular and phase properties [32].

In conclusion, our NMR investigations have proven that the slowing down of motions and changing of conformations make the mesomorphic molecular shapes organise within the smectic layers. The interplay of electric and packing interactions with translational and reorientational diffusion appears to be the driving force for inducing, from the relatively disordered behaviour of the molecules in the SmA phase, the changes generating the variety of characteristics observed for ferroelectric phases (and their analogues). Our findings suggest that these changes occur either continuously in the SmA phase until the SmC* phase is reached, or as a sudden process at the SmA–SmC* transition.

References

[1] Giocondo, M.; Jakli, A.; Saupe, A. *Eur. Phys. J. E* **2000**, *1*, 61–65.
[2] Jakli, A.; Saupe, A. *J. Appl. Phys.* **1997**, *82*, 2877–2880.
[3] Markscheffel, S.; Saupe, A. *Europhys. Lett.* **1996**, *36*, 691–694.
[4] Muševič, I.; Blinc, R.; Žekš, B. *The Physics of Ferroelectric and Antiferroelectric Liquid Crystals*; World Scientific Publishing Co. Pte. Ltd: Singapore, 2000.
[5] Lagerwall, S.T. *Ferroelectrics* **2004**, *301*, 15–45.
[6] Domenici, V.; Geppi, M.; Veracini, C.A. *Prog. Nucl. Magn. Reson. Spectrosc.* **2007**, *50*, 1–50 (and references therein).
[7] Saupe, A.; Englert, G. *Phys. Rev. Lett.* **1963**, *11*, 462–464.
[8] Domenici, V. *Pure Appl. Chem*. **2007**, *79*, 21–37.
[9] Veracini, C.A. In *Nuclear Magnetic Resonance of Liquid Crystals: NMR Spectra in Liquid Crystals the Partially Averaged Spin Hamiltonian*: Emsley, J.W., Ed.; Reidel: Dordrecht, 1985.
[10] Catalano, D.; Chiezzi, L.; Domenici, V.; Fodor-Csorba, K.; Dong, R.Y.; Geppi, M.; Veracini, C.A. *Macromol. Chem. Phys.* **2002**, *203*, 1594–1601.
[11] Catalano, D.; Cifelli, M.; Fodor-Csorba, K.; Gacs-Baitz, E.W.; Geppi, M.; Jakli, A.; Veracini, C.A. *Mol. Cryst. Liq. Cryst.* **2000**, *351*, 245–257.
[12] Catalano, D.; Cavazza, M.; Chiezzi, L.; Geppi, M.; Veracini, C.A. *Liq. Cryst.* **2000**, *27*, 621–627.
[13] Ragnoli, M. Masters Thesis, University of Pisa, Italy, 1999.
[14] Catalano, D.; Chiezzi, L.; Domenici, V.; Geppi, M.; Veracini, C.A. *J Phys Chem B.* **2003**, *107*, 10104–10113.
[15] Kaspar, M.; Hamplova, V.; Novotna, V.; Glogarova, M.; Pocieca, D.; Vanek, P. *Liq. Cryst.* **2001**, *28*, 1203–1209.
[16] Bubnov, A.; Domenici, V.; Hamplova, V.; Kaspar, M.; Veracini, C.A.; Glogarova, M. *J. Phys. Condens. Matter* **2009**, *21*, 035102-1-8.
[17] Chiezzi, L.; Domenici, V.; Dong, R.Y.; Geppi, M.; Veracini, C.A. *Chem. Phys. Lett.* **2002**, *358*, 257–262.
[18] Domenici, V.; Geppi, M.; Veracini, C.A. *Chem. Phys. Lett.* **2003**, *382*, 518–522.
[19] Catalano, D.; Cifelli, M.; Domenici, V.; Fodor-Csorba, K.; Richardson, R.; Veracini, C.A. *Chem. Phys. Lett.* **2001**, *346*, 259–266.
[20] Domenici, V.; Geppi, M.; Veracini, C.A.; Dong, R.Y. *Liq. Cryst.* **2006**, *33*, 479–484.
[21] Catalano, D.; Cifelli, M.; Geppi, M.; Veracini, C.A. *J. Phys. Chem. A* **2001**, *105*, 34–40.

[22] Dong, R.Y.; Zhang, J.; Veracini, C.A. *Solid State Nucl. Magn. Reson.* **2005**, *28*, 173–179.
[23] Dong, R.Y.; Chiezzi, L.; Veracini, C.A. *Phys. Rev. E: Stat., Nonlinear, Soft Matter Phys.* **2002**, *65*, 041716-1-7.
[24] Xu, J.; Dong, R.Y. *J. Phys. Chem. B* **2006**, *110*, 1221–1228.
[25] Xu, J.; Veracini, C.A.; Dong, R.Y. *Phys. Rev. E: Stat., Nonlinear, Soft Matter Phys.* **2005**, *72*, 051703-1-8.
[26] Cifelli, M.; Domenici, V.; Veracini, C.A. *Mol. Cryst. Liq. Cryst.* **2005**, *429*, 167–179.
[27] Domenici, V.; Geppi, M.; Veracini, C.A.; Zakharov, A.V. *J. Phys. Chem. B* **2005**, *109*, 18369–18377.
[28] Domenici, V.; Geppi, M.; Veracini, C.A.; Lebar, A.; Zalar, B.; Blinc, R. *Chem. Phys. Chem.* **2004**, *5*, 559–563.
[29] Zakharov, A.V.; Domenici, V.; Veracini, C.A.; Dong, R.Y. *Phys. Rev. E: Stat., Nonlinear, Soft Matter Phys.* **2006**, *73*, 011711-1-5.
[30] Zhang, J.; Domenici, V.; Veracini, C.A.; Dong, R.Y. *J. Phys. Chem. B* **2006**, *110*, 15193–15198.
[31] Zhang, J.; Domenici, V.; Dong, R.Y. *Chem. Phys. Lett.* **2007**, *441*, 237–244.
[32] Domenici, V.; Marini, A.; Veracini, C.A.; Dong, R.Y.; Zhang, J. *Chem. Phys. Chem.* **2007**, *8*, 2575–2587.
[33] Domenici, V.; Marini, A.; Menicagli, R.; Veracini, C.A.; Bubnov, A.; Glogarova, M. *Proc. SPIE* **2007**, *6587*, F1–F13.
[34] Dong, R.Y.; Geppi, M.; Marini, A.; Hamplova, V.; Kaspar, M.; Veracini, C.A.; Zhang, J. *J. Phys. Chem. B.* **2007**, *111*, 9787–9794.
[35] Domenici, V.; Marini, A.; Veracini, C.A.; Menicagli, R.; Malanga, C. *Chem. Phys. Chem.* **2009**, *10*, 2679–2691.
[36] Marini, A.; Domenici, V.; Veracini, C.A. Manuscript in preparation.
[37] Domenici, V. Masters Thesis, University of Pisa, Italy, 2001.
[38] Catalano, D.; Domenici, V.; Marini, A.; Veracini, C.A.; Bubnov, A.; Glogarova, M. *J. Phys. Chem. B* **2006**, *110*, 16459–16470.
[39] Frisch, M.J. *Gaussian 03 Revision B05*. Gaussian, Inc., Pittsburgh PA, 2003.
[40] Adamo, C.; Barone, V. *J. Chem. Phys.* **1998**, *108*, 664–675.
[41] Kaupp, M.; Malkin, V.G.; Bühl, M. *Calculation of NMR and EPR Parameters*; Wiley-VHC: Würzburg, Germany, 2004.
[42] Keith, T.A.; Bader, R.F.W. *Chem. Phys. Lett.* **1992**, *194*, 1–8.
[43] Dong, R.Y. *Nuclear Magnetic Resonance of Liquid Crystals*; Springer-Verlag: New York, 1997.
[44] Luckhurst, G.R.; Veracini, C.A. *The Molecular Dynamics of Liquid Crystals*; Kluwer Academic Publisher, 1989.
[45] Dong, R.Y. *Progr. Nucl. Magn. Reson. Spectrosc.* **2002**, *41*, 115–151.
[46] Fung, B.M. *Progr. Nucl. Magn. Reson. Spectrosc.* **2002**, *41*, 171–186.
[47] Abragam, A. *Principles of Nuclear Magnetism*; Oxford University Press: New York, 1961.
[48] Marini, A.; Prasad, V.; Dong, R.Y. In *Nuclear Magnetic Resonance Spectroscopy of Liquid Crystals*: Dong, R.Y., Ed.; World Scientific: Singapore, 2009.
[49] Dong, R.Y.; Marini, A. *J. Phys. Chem. B* **2009**, *113*, 14062–14072.
[50] Domenici, V.; Veracini, C.A. In *Nuclear Magnetic Resonance Spectroscopy of Liquid Crystals*: Dong, R.Y., Ed.; World Scientific: Singapore, 2009.
[51] Photinos, D.J.; Samulski, E.T. *Science* **1995**, *270*, 783–786.
[52] de Gennes, P.G.; Prost, J. *The Physics of Liquid Crystals*; Clarendon Press: New York, 1993.
[53] Zalar, B.; Gregorovic, A.; Simsic, M.; Zidaznek, A.; Blinc, R. *Phys. Rev. Lett.* **1998**, *80*, 4458–4461.
[54] de Gennes, P.G.; Prost, J. *The Physics of Liquid Crystals*; Clarendon Press: New York, 1993; pp 57–58.
[55] Englert, G.; Saupe, A. *Mol. Cryst. Liq. Cryst.* **1966**, *1*, 503–514.
[56] Domenici, V. Ph.D. Thesis, Università di Pisa, Italy, 2005.